ACI STRUCTURAL JOURNAL TECHNICAL PAPER

Title no. 96-S71

Cumulative Seismic Damage of Circular Bridge Columns: Benchmark and Low-Cycle Fatigue Tests

by Ashraf El-Bahy, Sashi K. Kunnath, William C. Stone, and Andrew W. Taylor

An experimental study was undertaken to investigate cumulative damage in reinforced concrete circular bridge piers subjected to a series of earthquake excitations. Twelve identical quarter-scale bridge columns, designed in accordance with current AASHTO specifications, were fabricated and tested to failure. This paper summarizes the results of Phase I testing that consisted of benchmark tests to establish the monotonic force-deformation envelope and the energy capacity under standard cyclic loads, and constant amplitude tests to determine the low-cycle fatigue characteristics of typical flexural bridge columns. A companion paper will present the results of variable amplitude testing that focused on the effects of load path on cumulative damage. Test observations indicate two potential failure modes: low cycle fatigue of the longitudinal reinforcing bars; and confinement failure due to rupture of the confining spirals. The former failure mode is associated with relatively large displacement amplitudes in excess of 4 percent lateral drift, while the latter is associated with a larger number of smaller amplitude cycles. A fatigue life expression is developed that can be used in damage-based seismic design of circular, flexural bridge columns.

Keywords: bridges (structures); cyclic loads; damage; ductility; earthquake-resistant structures; fatigue tests.

INTRODUCTION

Damage to bridge structures in past earthquakes has been significant. The 1971 San Fernando earthquake significantly damaged as many as 41 bridges. More recently, the 1989 Loma Prieta earthquake caused more than $5.5 billion in damage, of which almost a third was attributed to highway failures, the most notable being the collapse of a section of the Cypress viaduct.[1] Post-earthquake reconnaissance and follow-up research have indicated that most of the damage in highway bridges is a result of some or all of the following reasons: 1) insufficient column ductility and/or energy dissipation capacity to sustain the large imposed lateral displacements; 2) insufficient shear capacity in short columns; and 3) lack of adequate anchorage length in the longitudinal reinforcing bars of the piers.

The basic philosophy behind past and present AASHTO[2] or CALTRANS[3] specifications for the seismic design of bridge columns is based on a prescriptive approach; that is, the specifications place constraints on such factors as material properties, minimum reinforcement or confinement requirements, and column geometry, without specifically linking these requirements to the performance of the column when it is subjected to a particular earthquake. A designer who follows the prescriptive code requirements is ostensibly assured that the structural safety of the bridge pier will be preserved under maximum likely earthquakes at the bridge site. However, the designer cannot assess the degree and extent of damage suffered by the bridge column due to any magnitude of ground-shaking during its lifetime. The larger issue of seismic safety in future earthquakes, as well as the criteria to be used in upgrading, remains unresolved.

Much of the strength and deformation requirements in current highway bridge design procedures have been derived from experimental testing and limited analytical studies. However, it must be noted that most of the testing conducted in the past was directed towards the objective of understanding postyield behavior under cyclic load reversals to develop detailing strategies to insure satisfactory performance under seismic action. As such, these tests have provided pertinent knowledge regarding the effects of various important parameters, such as the influence of varying axial forces, the presence of high shear, confinement, and multidirectional loading, on the failure of bridge columns. Issues related to performance or correlation of observed behavior to damage have not been addressed directly; therefore, efforts related to calibrating damage models have not met with any success.

A major factor that has hindered the development of a performance-based design methodology is the fact that no systematic experimental program has yet been undertaken wherein the imposed loading, the system variables, and the measured or observed response were tailored to specifically monitor, model and calibrate cumulative seismic damage. The effort described in this paper is an initial step in this direction.

RESEARCH SIGNIFICANCE

This study is an attempt to understand the mechanics of cumulative damage in reinforced concrete bridge piers subjected to multiple earthquakes of varying magnitudes. The experimental program was designed to specifically address issues related to damageability and reserve capacity following a seismic event, and correlate observed damage with well-recognized damage parameters. It is the premise of this study that structural damage resulting from earthquake-induced forces is inextricably linked to the fatigue behavior of concrete and steel. The fatigue characteristics of typical flexural columns will provide a basis to develop a model of seismic structural damage for use in seismic performance assessment. This study is also concerned with identifying criteria for low-cycle fatigue failure of the column section on a general level with particular interest in the longitudinal reinforcing bar, and the role of confinement, as prescribed in modern codes, in altering flexural failure modes. Ultimately, the results of this study will contribute to the overall task of damage-based seismic design and the prediction of flexural failure modes in bridge columns.

SUMMARY OF PREVIOUS EXPERIMENTAL WORK

The earliest tests on bridge columns under simulated earthquake loads were carried out in Japan[4] and New Zealand.[5] The first shaking table study was conducted by

ACI Structural Journal, V. 96, No. 4, July-August 1999.
Received December 22, 1997, and reviewed under Institute publication policies.

ACI member **Ashraf El-Bahy** *is Senior Engineer at Tilden Lobnitz Cooper, Orlando, Fla. He received his PhD from the University of Central Florida, and his BS and MS in civil engineering from Cairo University, Egypt. His research interests include earthquake-resistant design of structures, and inelastic behavior and damage modeling of reinforced concrete.*

ACI member **Sashi K. Kunnath** *is Associate Professor of Structural Engineering at the University of Central Florida. He received his PhD in structural dynamics and earthquake engineering from the State University of New York, Buffalo, N.Y., and his MS from the Asian Institute of Technology. He is a member of ACI Committees 335, Composite and Hybrid Structures; 369, Seismic Repair and Rehabilitation; and 374, Performance-Based Seismic Design of Concrete Buildings. His research interests include inelastic behavior and damage-based design of concrete structural systems.*

William C. Stone *is Research Structural Engineer and Leader of the construction metrology and automation group at the National Institute of Standards and Technology, Gaithersburg, Md. He received his PhD from the University of Texas at Austin, Tex., and his BS and MS from Rensselaer Polytechnic Institute. His research interests include structural dynamics, real-time metrology, and robotics and automation in construction.*

ACI member **Andrew W. Taylor** *is Project Engineer with KPFF Consulting Engineers, Seattle, Wash. He is a member of ACI Committees 341, Earthquake-Resistant Concrete Bridges; and 374, Performance-Based Seismic Design of Concrete Buildings.*

Munro et al.[6] on a 1:6-scale model pier. Since then, a number of additional experiments have been carried out in Japan, New Zealand, and the U. S. on the inelastic shear and flexural behavior of bridge columns, the most significant of which are summarized as follows.

Mander et al.[7] tested the first large-scale square hollow bridge piers under lateral cyclic loading to establish the ductility capacity of hollow bridge piers that are commonly used in New Zealand. It was determined that the main parameter that controlled the ductility capacity of the columns was the amount of the lateral reinforcement. Another significant contribution of this particular work was the development of an analytical model leading to a better understanding of the role of confinement in seismic damage of reinforced concrete (RC) columns.

Full-scale and 1:6-scale model columns, which simulated both shear and flexural behavior, were tested at the National Institute of Standards and Technology to verify the adequacy of CALTRANS design specifications.[8,9] No significant drawbacks in the design were identified. Column tests dedicated to the study of shear behavior include the work of Ang et al.[10] and Wong et al.[11] The latter study focused on multidirectional loading, and concluded that biaxial loading patterns led to more severe stiffness degradation than uniaxially imposed loads.

Recently, Priestley and Benzoni[12] tested two large-scale circular columns with low longitudinal reinforcement ratios. One of the columns had 0.5 percent longitudinal reinforcement, while the second column had 1 percent, which represents 50 and 100 percent of the minimum reinforcement requirement of ACI, respectively. Both columns performed well, pointing to the possibility that the ACI minimum requirements for flexure can be further reduced. Additionally, there have been numerous tests conducted at the University of San Diego examining retrofit of columns and bridge bents.[13] Priestley et al.[14] tested a half-scale model of a typical section of a double-deck viaduct under simulated seismic loading. The 90,000-kg model was controlled by 14 hydraulic actuators and represents one of the most complex civil structures ever tested. The test was used to validate capacity design procedures that were proposed to retrofit existing double-deck bents in the California freeway system following the collapse of the Cypress viaduct in the 1989 Loma Prieta earthquake.

Hwang and Scribner[15] were the first, and perhaps only, investigators to study the effect of variations in displacement history. They clearly concluded that methods previously used to calculate energy dissipation capacity of members (for standard cyclic tests) did not consistently predict the cyclic capacity of a flexural member subjected to an arbitrary displacement history. This is despite the fact that the tests conducted by Hwang and Scribner were not truly random: they alternated cycles of low ductility with cycles of larger ductility demand.

The only work on low-cycle fatigue behavior of bridge columns is the experimental testing reported by Mander and Cheng[16] who investigated the applicability of specially detailed fuse bars in the plastic hinge region of the pier. The fatigue-based modeling reported in the study based on previous reinforcing bar fatigue tests conducted by Mander et al.[17] is an important development that shares the conceptual framework of the testing presented in this paper.

Table 1—Details of prototype and model

Item	Prototype	Model	Remarks
Longitudinal reinforcement	24 No. 11 (36 mm)	21 No. 3 (9.5 mm)	ρ = 2 percent
Spirals	No. 5 (16 mm)	Wire = 4-mm diameter	Smooth wire
Spiral pitch	76 mm	19 mm	$\rho_v = 0.1$
Spiral yield strength	414 MPa	380 to 450 MPa	—
Column diameter	1.22 m	0.3 m	Scale 1:4
Column length	5.5 m	1.37 m	Scale 1:4
Cover	50 mm	12.5 mm	Scale 1:4
Embedment length of bars	Tension = 1.4 m Compression = 0.72 m	Tension = 0.35 m Compression = 0.18 m	—
Axial load	3225 kN	806 kN	$0.1 f'_c A_g$
Lateral load capacity	1550 kN	388 kN	$V_p = M_p/H$
Spacing of longitudinal steel	100 mm	25 mm	—

DETAILS OF EXPERIMENTAL PROGRAM

The test program was designed to keep material, geometric, and section variables to a minimum. Since different failure modes may result in different critical damage parameters, only flexural failure modes were considered in this study. The experimental program consisted of tests on 12 quarter-scale, circular, reinforced concrete columns. In keeping with the main objectives of the study, the primary variables considered were the amplitude, sequence and type of loading pattern. The tests were conducted in two phases. Phase I testing, reported in this paper, consisted of benchmark tests that included characterization of the fatigue behavior of the model columns. In Phase II, another set of six identical specimens were subjected to random displacement histories, the details of which are described in a companion paper.

The full-scale single-bent pier on which the model column was designed conforms to the specifications of AASHTO.[2] A quarter-scale model was selected as an appropriate size within the limits of the testing capabilities available, and for which no special modeling treatment of the constituent materials (with the exception of the hoop steel) was necessary. Only dimensional scaling was used. Material properties were selected to match those of the prototype. Table 1 shows the dimensions, reinforcement details, applied axial load and lateral load capacity for both the prototype and the model. Dimensional and reinforcement details of the specimen are shown in Fig. 1.

Material properties

The steel used for the main longitudinal bars of the columns was Grade 60 reinforcing bars with an average yield strength of 470 MPa. At a scale of 1:4, the model pier required 9.5-mm (No. 3) bars conforming to ASTM A 615-90, which was not a

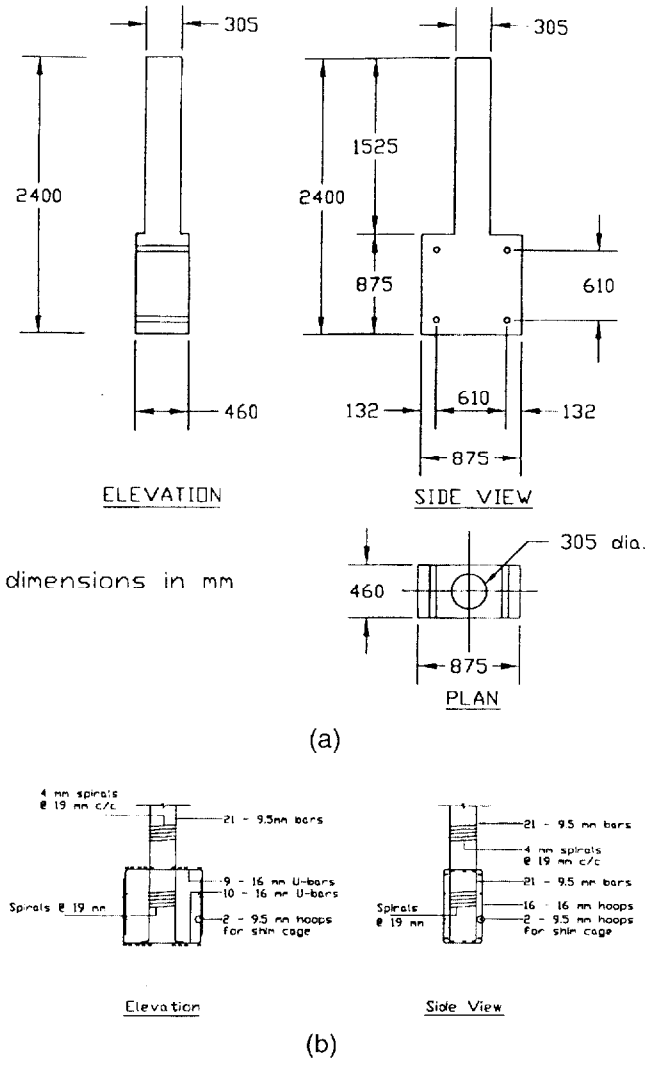

Fig. 1—Specimen details: (a) configuration and dimensions; and (b) reinforcement.

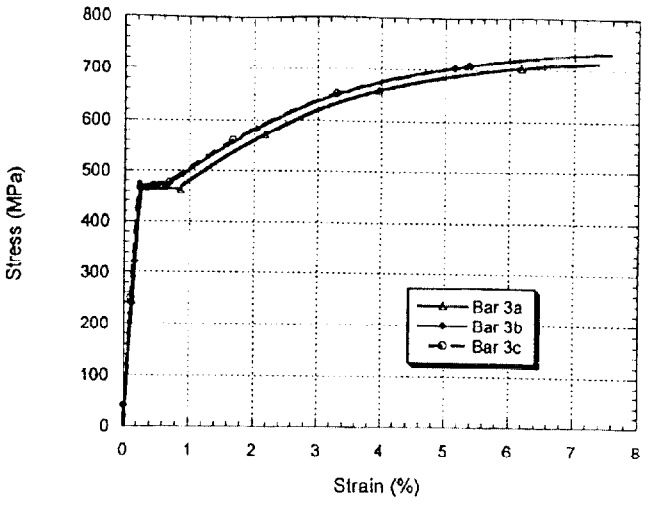

Fig. 2—Stress-strain profile of main No. 3 longitudinal bars.

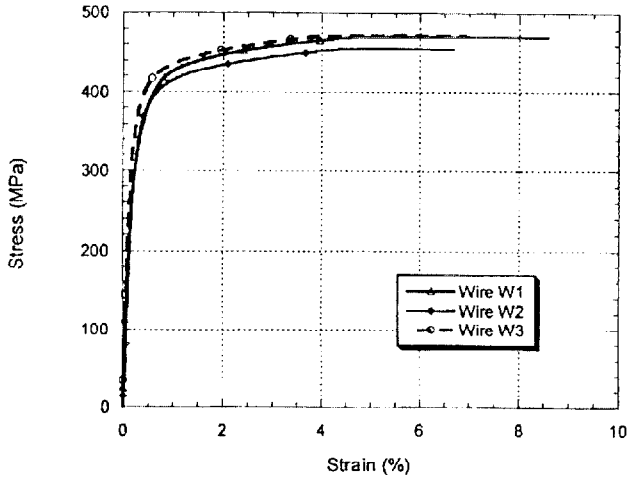

Fig. 3—Stress-strain profile of annealed hoop reinforcement.

problem since this size is commercially available. Fig. 2 shows typical stress-strain curves of the No. 3 bars used as main longitudinal reinforcement. However, for the hoop reinforcement, the dimensional scaling resulted in the use of 4-mm-diameter wires. Commercially available gage wire had to be annealed through carefully controlled heat treatment. The heat treatment produced an average wire yield strength of 408 MPa, which was comparable to Grade 60 bars, though the strain-hardening characteristics were different. Fig. 3 displays the achieved stress-strain behavior of the annealed wire used as confining spirals.

The stress-strain curves presented in Fig. 2 and 3 do not include the fracture strain. The extensometers used to measure the specimen elongation had to be removed prior to fracture to prevent damage to the instrument. However, the total elongation of the gage length was measured, the resulting final strain was calculated, and these results are tabulated in Table 2. The energy to fracture was computed by assuming that the stress-strain diagram was linear from the last instrumented strain reading to the fracture strain. Assuming that a typical hoop bar exhibits characteristics similar to a 9.5- or a 16-mm (No. 3 or 5) bar, yield strength and ductility parameters obtained for the annealed steel wire may be considered acceptable, even though the fracture energy exhibits variations up to 20 percent. The significance of this difference in predicting the fatigue life of RC columns is discussed in the concluding sections of both papers.

The columns were poured monolithically with the footings. The concrete used in the construction had an average slump of 200 mm and a maximum aggregate size of 12.5 mm. The specimens were cast in two batches of six specimens each. The specified mix proportions resulted in an average concrete strength of 36 MPa for the first batch, and 40.1 MPa for the second batch, as measured at the time of testing.

Setup and instrumentation

The test setup was assembled from standard steel wide-flanged sections. Lateral bracing was provided in the direction of the applied load, and two steel beams with smooth surface plates were attached to the testing frame on either side of the specimen parallel to the direction of loading to prevent any out-of-plane displacement during testing. Rollers were attached to the column head to permit relatively friction-free movement. The final setup with the specimen in place and the test apparatus, but without the out-of-plane support system, is shown in Fig. 4. Note that the foundation block is composed of three parts: the midsection is cast as part of the pier, while the side blocks were cast separately as reusable end blocks that were connected to the specimen through post-tensioning. The foundation block of the specimen, as poured in-place, measures approximately 460 x 875 mm. However, once the side blocks are attached and post-tensioned, the width of the foundation in the direction of loading is approximately 2.0 m. The use of

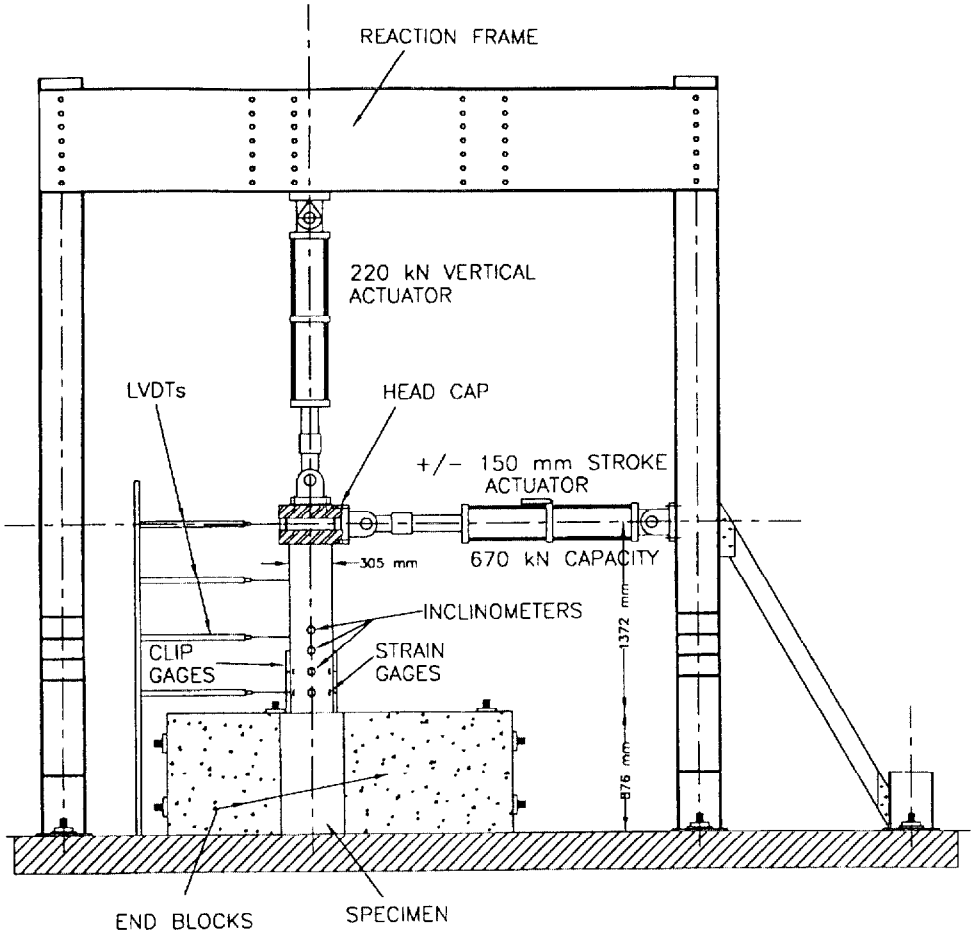

Fig. 4—Test setup and instrumentation.

Table 2—Summary of reinforcing bar characteristics

Specimen		f_y, MPa	E_s, MPa	f_{su}, MPa	ε_{su}, percent	ε_{sf}, percent	E_{fr}, MPa
Group	No.						
No. 3 reinforcing bar	3a	463	213,500	733	8.5	14.6	99.25
	3b	472	215,900	714	9.7	13.8	90.95
	3c	476	227,300	723	7.9	15.7	106.59
4-mm-diameter wire	W1	419	234,600	471	—	17.5	80.44
	W2	407	210,900	455	—	19.1	85.01
	W3	398	216,100	475	—	16.9	78.40
No. 5 reinforcing bar	5a	422	220,600	650	8.2	16.9	102.70
	5b	430	226,100	664	7.7	17.3	105.80
	5c	423	203,200	656	8.3	16.2	97.72

Notations: f_y = yield stress; E_s = Young's modulus; f_{su} = ultimate (peak) stress; ε_{su} = strain at peak stress; ε_{sf} = fracture strain; and E_{fr} = fracture energy.

post-tensioned blocks considerably reduced the amount of concrete required to construct each specimen.

The lateral displacement was applied by a servo-controlled 670-kN MTS hydraulic actuator with a stroke of ±150 mm. The applied lateral displacement and load were measured using a calibrated linear variable displacement transducer (LVDT) and load cell, respectively. On the opposite side of the loading actuator, a string potentiometer and two LVDTs were mounted against the specimen to measure the lateral displacement of the specimen at different elevations. The string potentiometer was placed at the same level of the actuator centerline: 1370 mm from the top of the footing. The two LVDTs were placed at 455 and 910 mm from the top of the footing. The vertical load was applied using a 220-kN servo-controlled MTS ram. The vertical load was recorded using the calibrated load cell of the actuator. The applied vertical load during testing was approximately constant at $0.1f'_cA_g$, which is the estimated weight of the bridge deck.

The curvature in the plastic hinge region was calculated using six clip gages mounted on opposite sides of the specimen in a plane parallel to the loading direction. The clip gages consisted of two strain gages mounted on light-gage C-shaped steel sections that, in turn, were hooked between two points on the specimen equal to the gage length L. The curvature was calculated using the following expression

$$\Phi = \frac{(\Delta_2 - \Delta_1)}{Lx} \quad (1)$$

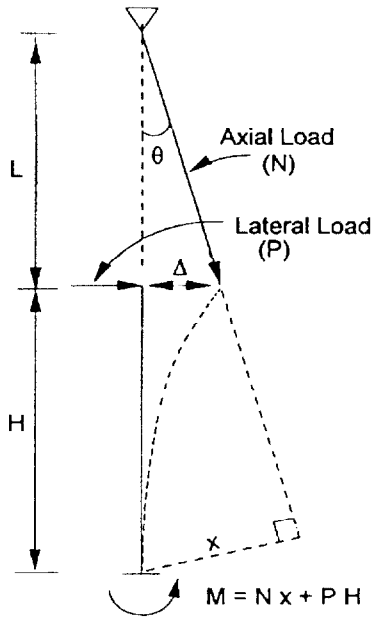

Fig. 5—Forces on specimen and computation of shear with P-delta effects.

where

Δ_1 = contraction or expansion measured by Clip Gage 1;

Δ_2 = expansion or contraction measured by the opposite Clip Gage 2;

L = gage length; and

x = distance between the gage mount points.

The previous equation is generally valid only under the assumed condition that plane sections remain plane after bending. Curvature measurements beyond yield were also affected by spalling of the cover concrete.

Four clinometers were mounted on the specimen, as shown in the figure, to measure the angle of rotation at the base of the column during testing. The clinometers were connected to a special base, which in turn was connected to threaded rods that were embedded inside the specimens. The clinometers were attached to the specimen at 150, 300, 450, and 600 mm, respectively, from the base of the column (top of the footing).

Finally, four strain gages were installed on each specimen: two each on opposite longitudinal reinforcing bars in the loading plane. The strain gages were installed at 100 and 200 mm from the base of the column. These locations were based on estimates of the plastic hinge length of the specimen after yielding. The strain gage readings were used to check the initiation of yielding and the spread of plasticity.

RESULTS OF PHASE I TESTING

Six specimens (labeled A1 to A6) were tested in this phase. Benchmark tests were conducted to obtain relevant force-deformation and low-cycle fatigue characteristics of the specimen. As will be shown later, these response parameters are critical to developing damage-based performance criteria.

1. *Monotonic loading (Specimen A1)*—The purpose of this test is to develop the backbone force-deformation envelope for the specimen. Some damage models use strength and deformation quantities derived from a monotonic test to normalize and/or formulate damage expressions.

2. *Standard cyclic test (Specimen A2)*—This was considered essential since all past laboratory testing has been based on this approach. This would provide a convenient benchmark against which to compare random amplitude testing.

3. *Low-cycle fatigue testing (Specimen A3 to A6)*—In an attempt to calibrate fatigue-based damage models for flexural members, these tests provided the basis for developing a fatigue-life expression for the specimen.

Records kept during testing included information such as crack widths, spalling, exposed reinforcement, etc. that permit calibration of damage to visual observations in post-earthquake reconnaissance. Failure was typically defined by either the rupture of confining spirals or fracture of longitudinal reinforcing bars. Other essential details, such as necking of hoops or buckling of longitudinal bars, were also monitored.

The recorded force-deformation data was converted to shear versus displacement response, taking into consideration the additional moments induced due to P-delta effects. Fig. 5 shows a schematic diagram of the test setup and the relevant quantities required to derive the necessary forces and moments. With reference to Fig. 5, the shear force V in the column is given by

$$V = P + \frac{Nx}{H} \tag{2}$$

where

$$x = (L + H)\sin\theta \tag{3}$$

and

$$\theta = \tan^{-1}\left(\frac{\Delta}{L}\right) \tag{4}$$

Benchmark tests

Monotonic test—Specimen A1 was tested under a monotonically increasing lateral load until failure. Spalling of the concrete cover was observed at approximately 35-mm (2.5 percent drift) lateral displacement. The maximum lateral load reached 66 kN before additional displacement caused a gradual softening of the column stiffness. Two longitudinal bars showed signs of buckling as the lateral load capacity of the specimen began to drop at a drift of approximately 4.0 percent. The definition of failure in a monotonic test is difficult to establish; while it is conceivable that large lateral displacements (without reversals) can strain the longitudinal bars to fracture, such a level of displacement was not possible in the present test, given the limitation of stroke capacity of the hydraulic actuator. Additionally, at these large displacements, P-delta effects are significant and the resulting secondary moments can result in collapse of the structure. Again, the test setup, consisting of hydraulic actuators mounted directly onto the specimen, will prevent this from happening. Given these circumstances, it was decided to stop testing at a lateral drift of 11 percent, at which state P-delta collapse was considered to be the possible failure mode. Fig. 6 shows the resulting force-deformation envelope.

Standard cyclic test—Specimen A2 was subjected to three cycles each at lateral displacement amplitudes of 1.0, 1.5, 2.0, 2.5, 3.0, 4.0, 5.0, and 6.0 percent until failure [Fig. 7(a)]. A smaller displacement cycle of 0.5 percent drift was applied between each increase in amplitude to monitor changes in the specimen stiffness. Crack widths up to 1.5 mm were measured at Cycle 19 when the drift was approximately 3 percent. Yielding of the extreme longitudinal bar was estimated at a displacement of 20 mm when the lateral load reached approximately 65 kN. Spalling of the concrete cover was observed at Cycle 15 at a drift of approximately 3 percent. Significant cracking propagated up to 225 mm beyond the base of the column at this stage. Minor bar buckling and significant spalling was evident by the end of Cycle

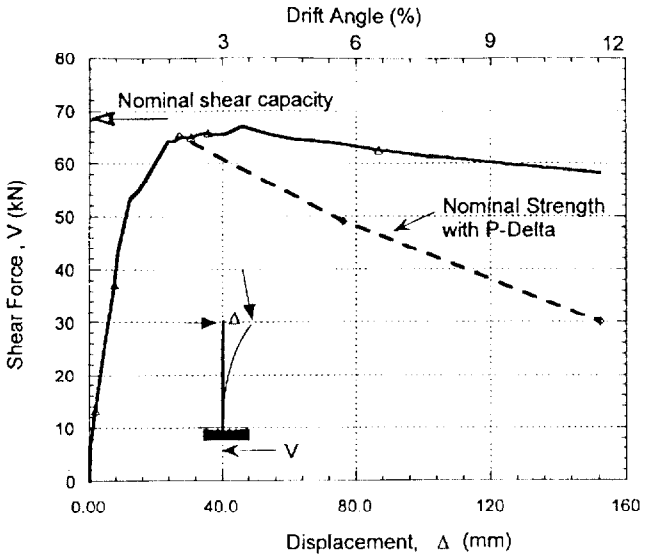

Fig. 6—Response of column to monotonic loading.

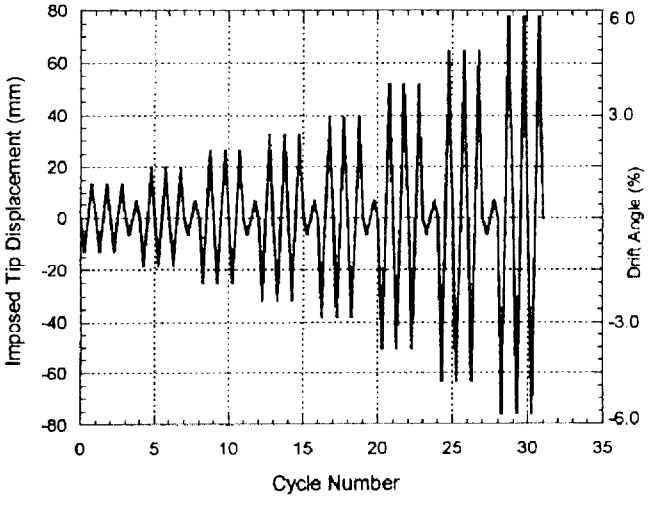

(a)

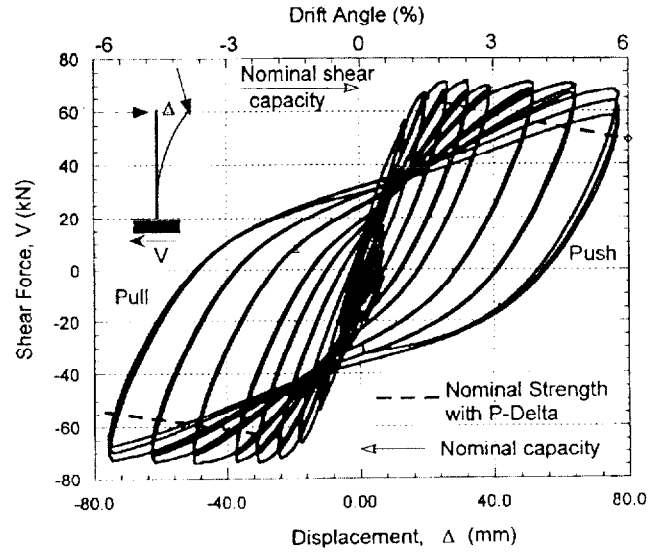

(b)

Fig. 7—Response of bridge column to standard cyclic loading: (a) imposed displacement history, and (b) load-deformation behavior.

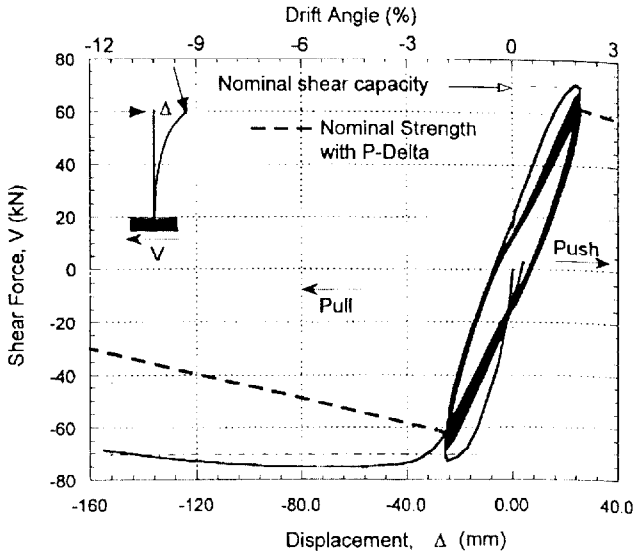

Fig. 8—Shear versus deformation response of specimen subjected to 2 percent constant amplitude cycling followed by monotonic push to failure.

22 at an imposed drift of 4.0 percent. Failure of the specimen occurred at a drift of approximately 5.5 percent following rupture of the confining spiral in the plastic hinge zone. The plastic hinge length was estimated as 180 mm, though cracking propagated beyond this region. The recorded shear force versus lateral displacement of the specimen is displayed in Fig. 7(b).

Low-cycle fatigue tests

Specimen A3 was subjected to constant amplitude cycles at a displacement amplitude corresponding to 2 percent lateral drift. After 40 complete cycles at a constant displacement amplitude of ±26 mm, no visible deterioration of the specimen was observed. The maximum measured crack widths on either side were approximately 0.8 to 1.0 mm. Loading of the specimen continued over a two-day period for 150 cycles without any further visible damage. Later, it was analytically estimated that this specimen would have sustained approximately 400 or more cycles. Since one of the objectives of the test program was to evaluate different damage models, it was decided that the cyclic loading could be discontinued and a monotonic load applied until failure. This would provide information on reserve capacity that is crucial to many damage modeling theories. The specimen sustained a final drift amplitude of almost 10 percent. Results of the observed force-displacement response are presented in Fig. 8.

Specimen A4 was subjected to repeated cyclic loading at a constant displacement amplitude of ±57 mm until failure. This displacement was equal to a drift of approximately 4.0 percent. On the very first cycle, spalling of the cover concrete was observed on the compression side of the specimen. By the third cycle, spalling had progressed to approximately 150 mm on both sides of the specimen. At the end of Cycle 8, the plastic hinge stabilized at approximately 150 to 160 mm. Buckling of longitudinal bars was observed on both sides of the specimen after 17 cycles. This led to necking of the confining spiral reinforcement. Failure of the specimen occurred at Cycle 26, following the rupture of a spiral approximately in the middle of the plastic hinge zone on the tension side. The recorded shear force versus lateral displacement response history for Specimen A4 is shown in Fig. 9.

Specimen A5 was tested under repeated cyclic loading at a constant amplitude of ±75 mm, corresponding to a drift of approximately 5.5 percent. Cracking of the concrete, yielding of the longitudinal reinforcement, and spalling of the cover con-

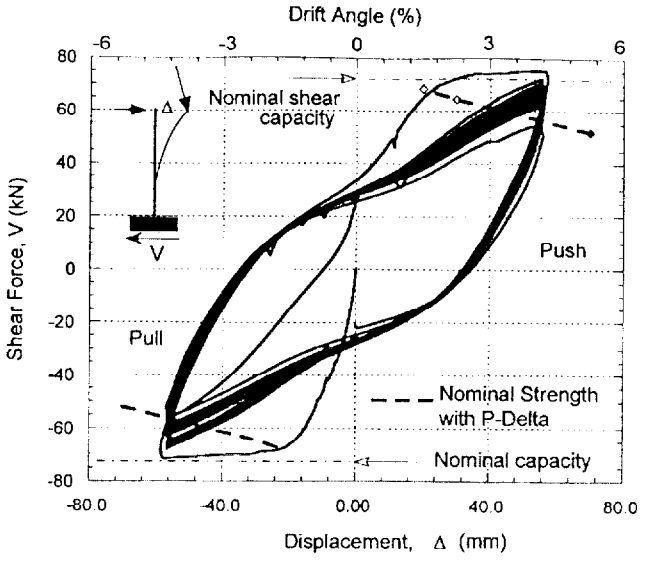

Fig. 9—Response to constant amplitude cycling at 4.0 percent lateral drift.

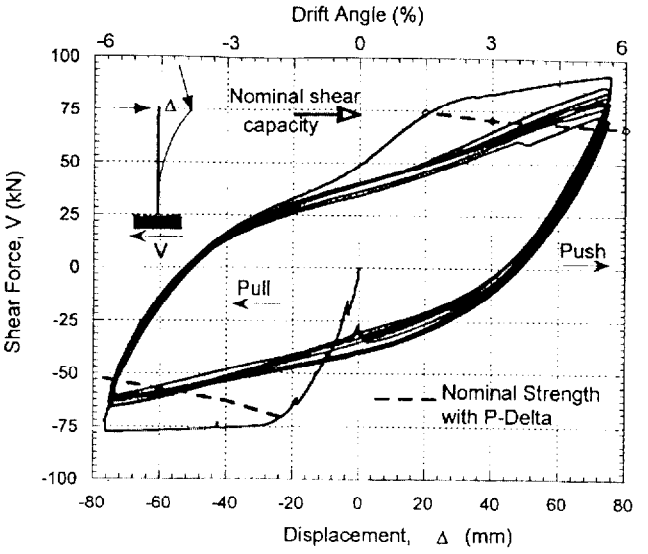

Fig. 10—Shear displacement response of column to 5.5 percent constant amplitude cycling.

crete were all observed in the very first push to the peak displacement. Significant buckling of longitudinal bars was observed on both sides of the specimen at Cycle 9. The plastic hinge length was approximated as 175 mm. The specimen failed through fracture of a longitudinal bar before the completion of Cycle 10. The complete load-deformation history of the specimen is plotted in Fig. 10.

The final specimen (A6) to be tested under constant amplitude loading was subjected to a displacement amplitude of ± 95 mm, corresponding to approximately 7 percent drift. The damage progression was similar to Specimen A5. The plastic hinge length, however, was much longer, reaching a total length of almost 250 mm. During the third cycle, hoop failure was initiated by a spiral rupture (followed by the fracture of a longitudinal bar) leading to a dramatic decay in load-carrying capacity, as is evident from the load-deflection plot shown in Fig. 11.

FATIGUE LIFE RELATIONSHIP

A more complete understanding of the cumulative damage process is possible with the establishment of a fatigue life relationship for the columns evaluated in this experimental study. The most widely used fatigue life equations are adopted from the following form of the Coffin-Manson[18,19] expression

$$\varepsilon_p = \varepsilon'_f (N_{2f})^c \tag{5}$$

where

ε_p = plastic strain amplitude;
ε'_f = a material constant to be determined from fatigue testing;
N_{2f} = number of complete cycles to failure; and
c = material constant to be determined.

A similar expression more suitable for structural components was suggested by Krawinkler et al.,[20] as follows

$$N_{2f} = C^{-1}(\Delta\delta_p)^{-c} \tag{6}$$

where $\Delta\delta_p$ is the plastic deformation and c and C are material constants to be determined experimentally.

The results of the constant amplitude tests were utilized in a curve-fitting exercise using a format similar to Eq. (5) and (6) that yielded the following relationship

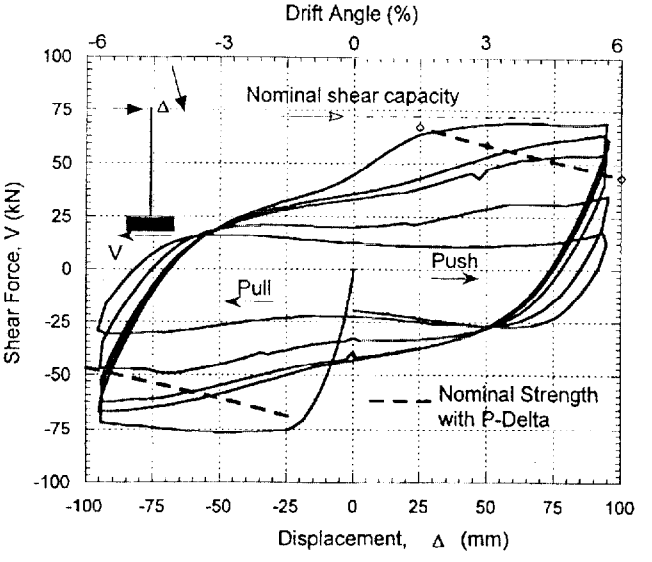

Fig. 11—Response of column to low-cycle fatigue loading at constant drift amplitude of 7.0 percent.

$$\delta, \text{percent} = 10.6(N_{2f})^{-0.285} \tag{7}$$

where δ is the lateral drift.

The plot of the previous expression shown in Fig. 12 indicates that experimentally observed values lie reasonably close to the proposed fatigue-life line, despite the fact that only three points were used to construct the expression. The fourth point corresponding to Specimen A3 was extrapolated theoretically, using Eq. (5). This fatigue-life equation will be utilized to predict the damage sustained by a second series of columns subjected to random amplitude loading and is reported in a companion paper.

SUMMARY OF FINDINGS

At the outset, it must be mentioned that this research investigation was limited to the study of circular columns with a predominantly flexural response. Circular sections have the advantage of possessing fairly uniform properties in any direction, and are commonly used in bridge construction, particularly in seismic zones. The observations, find-

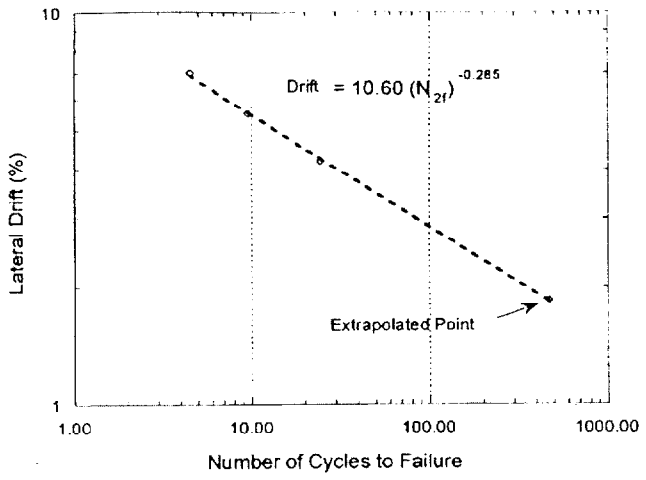

Fig. 12—Fatigue life relationship for flexural columns.

ings, and conclusions are therefore limited to seismically detailed flexural circular columns only. Failure, as defined in this study, is restricted to damage to the bridge pier only. Other potential damage sources, such as foundation failure and deck-abutment connection failures, are beyond the scope of this investigation.

1. Three potential failure modes were identified (Fig. 13): the first is essentially a precursor to the ultimate failure mode and consists of global buckling of the longitudinal bars that occurs over a length corresponding to several hoop spaces; the second failure mode is a result of confinement failure following the rupture of the transverse hoop steel; and the third observed mode of failure, typically associated with large displacements, is a low-cycle fatigue fracture of a longitudinal bar.

2. There exists a threshold ductility level for well-confined flexural circular columns designed by current CALTRANS (or AASHTO) specifications beyond which severe degradation of stiffness and strength takes place. For the bridge columns tested in this study, this threshold displacement ductility level occurs between $3\Delta_y$ and $4\Delta_y$, which corresponds to a lateral drift between 4 and 5 percent. Specimen A3, which was cycled 150 times at 2 percent drift, showed virtually no signs of damage or deterioration. Specimen A5, which was cycled at a lateral drift of 5.5 percent, failed in less than 10 cycles. It may, therefore, be stated that earthquakes that impose displacement ductility demands less than 2.0, bridge columns can survive a series of similar events without undergoing any significant structural damage. When the ductility demand approaches 4.0, the likelihood of moderate to severe damage is high and depends on the number of such inelastic cycles experienced by the structure. Further, it is estimated that the yield displacement (Δ_y) for the prototype column is approximately 1.5 percent, assuming that the force-deformation backbone envelope is idealized as a bilinear function.

3. Under a sequence of predominantly low amplitude cycles, it is more probable that the confining spiral will fail prior to low-cycle fatigue failure of the longitudinal reinforcing bars. Conversely, if the bridge column is subjected to predominantly high amplitude inelastic cycles, it is more likely that the longitudinal bars will rupture before confinement failure occurs. In the present study of flexural columns, it was found that the threshold low-amplitude cycle is approximately 2 to 4 percent drift, while high-amplitude cycles are those in excess of 4 percent drift. It must be added that this finding may contradict the observation of hoop failure in Specimen A6; however, fatigue cracks were also initiated in the longitudinal bars. A possible explanation for premature hoop failure is the fact that the fracture energy capacity of the annealed wires is less than that for comparable normal deformed reinforcement (Table 2).

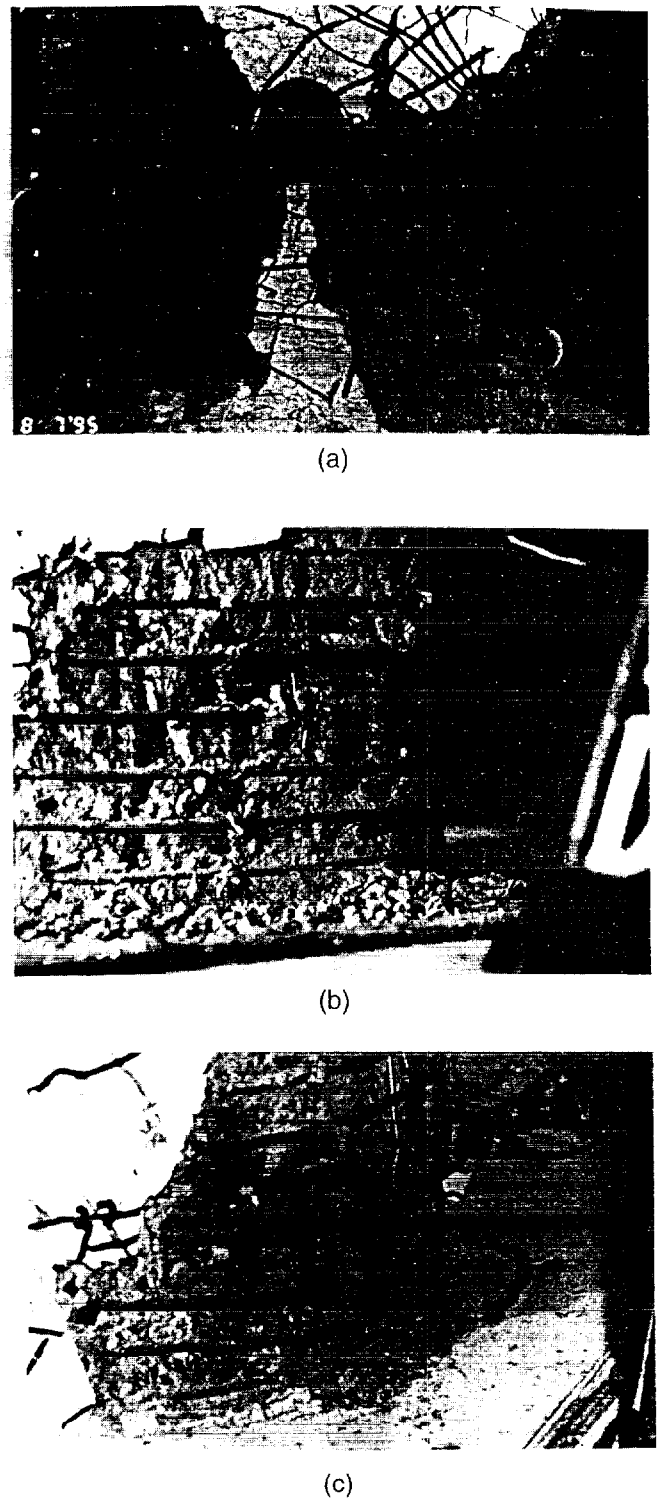

Fig. 13—Typical failure modes: (a) longitudinal bar buckling; (b) hoop fracture; and (c) low-cycle fatigue failure of longitudinal bar.

4. The tests also revealed that the energy capacity of a member at failure is dependent on the drift amplitude. Fig. 14 summarizes the dissipated hysteretic energy of each of the six specimens. The energy capacity clearly decays with drift amplitude.

5. The findings and observations from this phase of testing will be utilized in a study of cumulative damage resulting from random amplitudes that are more characteristic of earthquake-imposed loading, and will be presented in a companion paper.

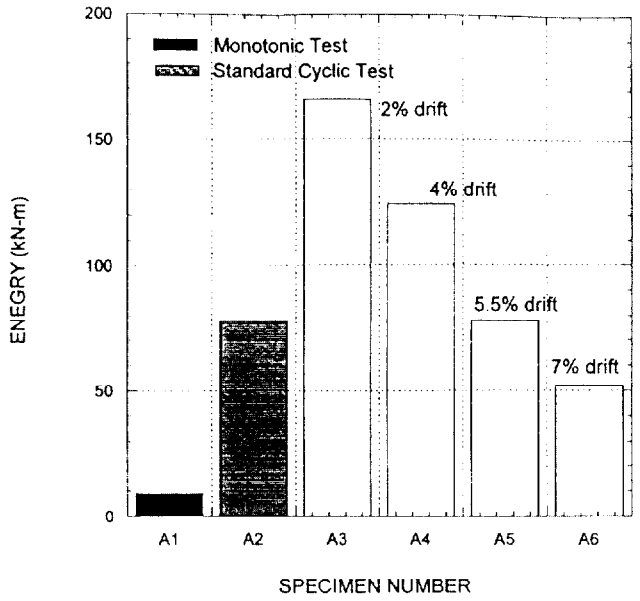

Fig. 14—Energy capacity of specimens at failure.

ACKNOWLEDGMENTS

Financial support for this project provided by the National Center for Earthquake Engineering Research (NCEER), the Federal Highway Administration (FHWA), and the California Department of Transportation (CALTRANS) is gratefully acknowledged. Special thanks are due to the technical staff of the Structural Testing Laboratory at the National Institute of Standards and Technology: Steve Johnson, Frank Rankin, Erik Anderson, Max Peltz, and James Little for their assistance with the experimental testing.

CONVERSION FACTORS

1 mm	=	0.0394 in.
1 m	=	3.28 ft
1 mm^2	=	0.00155 in.^{2}
1 MPa	=	145 psi
1 kN	=	0.225 kip-force

NOTATIONS

A_g	=	gross area of column section
E_{fi}	=	fracture energy
E_s	=	Young's modulus
f'_c	=	unconfined concrete compressive stress
f_{su}	=	ultimate (peak) stress
f_y	=	yield stress
H	=	height of column
M_p	=	nominal moment capacity of column
N	=	axial load in column
N_{2f}	=	number of complete cycles to failure
P	=	applied shear force on specimen
V	=	shear force in column
x	=	distance between gage mount points
Δ_1	=	contraction or expansion measured by Clip Gage 1
Δ_2	=	expansion or contraction measured by opposite Clip Gage 2
ε'_f	=	material constant to be determined from fatigue testing
ε_p	=	plastic strain amplitude
ε_{su}	=	strain at peak stress
ε_{sf}	=	fracture strain
ρ	=	longitudinal reinforcement ratio

REFERENCES

1. Office of Planning and Research, "Competing Against Time," *Report* to Governor George Deukmejian from the Governor's Board of Inquiry on the 1989 Loma Prieta Earthquake, G. W. Housner, ed., State of California.

2. AASHTO, "Standard Specifications for Highway Bridges," 14th edition, American Association of State Highway and Transportation Officials (AASHTO), Washington, D.C., 1989.

3. CALTRANS, "Bridge Design Specifications," State of California Department of Transportation, Office of Structure Design, Sacramento, Calif., 1992.

4. Building Research Institute, "A Seismic Analysis of Building Structural Members: List of Experimental Results on Deformation Ability of Reinforced Concrete Column under Large Deflection," BRI, Ministry of Construction, Japan, No. 3, 1975 and 1978, 182 pp.

5. Davey, B. E., "Reinforced Concrete Bridge Piers under Seismic Loading," master's *report*, University of Canterbury, Christchurch, New Zealand, Feb. 1975.

6. Munro, I. R. M.; Park, R.; and Priestley, M. J. N., "Seismic Behavior of Reinforced Concrete Bridge Piers," *Report* No. 76-9, University of Canterbury, Christchurch, New Zealand, 1976.

7. Mander, J. B.; Priestley, M. J. N.; and Park, R., "Seismic Design of Bridge Piers," *Research Report* No. 84-2, University of Canterbury, Christchurch, New Zealand, 1984.

8. Stone, W. C., and Cheok, G. S., "Inelastic Behavior of Full-Scale Bridge Columns Subjected to Cyclic Loading," *NIST Building Science Series Report* No. 166, U.S. Department of Commerce, National Institute of Standards and Technology, Gaithersburg, Md., 1989, 252 pp.

9. Cheok, G. S., and Stone, W. C., "Behavior of 1/6 Scale Model Bridge Columns Subjected to Cyclic Inelastic Loading," *Report* No. NBSIR 86-3494, U.S. Department of Commerce, National Institute of Standards and Technology, Gaithersburg, Md., 1986, 270 pp.

10. Ang, B. G.; Priestley, M. J. N.; and Paulay, T., "Seismic Shear Strength of Circular Bridge Columns, *Research Report* No. 85-5, University of Canterbury, Christchurch, New Zealand, 1985, 408 pp.

11. Wong, Y. L.; Paulay, T.; and Priestley, M. J. N., "Response of Circular Columns to Multi-Directional Seismic Attack, *ACI Structural Journal*, V. 90, No. 2, Mar.-Apr. 1993, pp. 180-191.

12. Priestley, M. J. N., and Benzoni, G. "Seismic Performance of Circular Columns with Low Longitudinal Reinforcement Ratios," *ACI Structural Journal*, V. 93, No. 4, July-Aug. 1996, pp. 474-485.

13. Priestley, M. J. N., Seible, F; Xiao, Y.; and Verma, R., "Steel Jacket Retrofitting of Reinforced Concrete Bridge Columns for Enhanced Shear Strength—Part 2: Test Results and Comparison with Theory," *ACI Structural Journal*, V. 91, No. 5, Sept.-Oct. 1994, pp. 537-551.

14. Priestley, M. J. N.; Seible, F.; and Anderson, D. L., "Proof Test of Retrofit Concept for San Francisco Double-Deck Viaducts: Part 2—Test Details and Results," *ACI Structural Journal*, V. 90, No. 6, Nov.-Dec. 1993, pp. 616-631.

15. Hwang, T. H., and Scribner, C. F., "RC Member Cyclic Response during Various Loadings," *Journal of Structural Engineering*, ASCE, V. 110, No. 3, 1984, pp. 466-489.

16. Mander, J. B., and Cheng, C.-T., "Renewable Hinge Detailing for Bridge Columns," *Pacific Conference on Earthquake Engineering*, Melbourne, Australia, Nov. 20-22, 1995.

17. Mander, J. B.; Panthaki, F. D.; and Kasalanati, A., "Low-Cycle Fatigue Behavior of Reinforcing Steel," *Journal of Materials in Civil Engineering*, ASCE, V. 6, No. 4, 1994.

18. Coffin, L. F., Jr., "A Study of Effects of Cyclic Thermal Stresses on Ductile Metal," *Transactions of the American Society of Mechanical Engineers*, New York, 76, 1954, pp. 931-950.

19. Manson, S. S., "Behavior of Materials under Conditions of Thermal Stress," *Heat Transfer Symposium*, University of Michigan Engineering Research Institute, Ann Arbor, Mich., 1953, pp. 9-75.

20. Krawinkler, H. et al., "Recommendations for Experimental Studies on Seismic Behavior of Steel Components and Materials," *John Blume Center Report* No. 61, Stanford University, Calif., 1983.

ACI STRUCTURAL JOURNAL TECHNICAL PAPER

Title no. 96-S72

Influence of Interfacial Shear Transfer on Behavior of Concrete-Filled Steel Tubular Columns

by Andrew E. Kilpatrick and B. Vijaya Rangan

As part of a research program on the behavior under load of high-strength concrete-filled steel tubular (CFST) columns, a series of tests has been undertaken to study the influence of the shear transfer by bond between the infill concrete and the inner surface of the circular steel tube. Three different cases of bond were examined together with four different loading regimes and slenderness ratios. Companion tests on similar empty steel tubes were also undertaken to highlight the synergistic effect of the steel and concrete acting compositely together. Conclusions are drawn on the significance of bond in the columns tested in this investigation.

Keywords: columns (supports); composite construction (concrete and steel); high-strength concretes.

INTRODUCTION

Concrete-filled steel tubular (CFST) columns offer a number of advantages in both design and construction. The steel tube: (1) acts as permanent formwork for the plastic concrete; (2) provides well-distributed reinforcement in the most efficient position to resist applied bending moments; (3) confines the hardened concrete, which increases its strain capacity and strength; and (4) protects the surface of the concrete from physical damage and deleterious environmental effects, such as carbonation. In turn, the concrete increases the critical buckling stress of the (imperfect) steel tube by changing its buckling mode, particularly so for noncircular sections. Overall, composite column construction: (1) improves the speed of construction; (2) reduces the cross-sectional dimensions of the column for a given column strength, thereby making more floor area available for occupants' use; (3) encourages the use of simple connections to steel floor beams, which reduces the design time; (4) offers higher impact resistance and considerable toughness; and (5) improves overall member ductility. Some disadvantages include a reduced resistance to fire, and connections between the steel floor beams and tubular columns sometimes being limited to simple joints because of the difficulty of achieving full moment continuity.

Nonetheless, in the many situations, the advantages offered by CFST columns outweigh their disadvantages. Consequently, this form of construction has enjoyed an increase in popularity in recent years, and has been used primarily as columns supporting platforms in offshore structures, roofs of oil storage tanks, columns for large industrial workshops and open-air overhead travelling cranes, as well as piles and piers for bridges and viaducts. Their use as columns in multistory buildings has increased in recent years as the benefit of increased load-carrying capacity for a reduced cross section, resulting in an increase in net floor space, has been realized. Because of their excellent ductility, CFST columns have also been used in earthquake resistant structures, particularly in Japan.

RESEARCH SIGNIFICANCE

One of the concerns associated with composite columns is the influence of the bond between the inside of the steel tube and the infill concrete upon the behavior under load of both stub columns and slender columns alike. Recently, a comprehensive series of pushout tests on stub columns has been reported.[1,2] However, little work has been undertaken on the influence of bond upon the load-deformation response and strength of slender and stocky composite columns; this is the subject of the work summarized here and fully reported elsewhere.[3]

TEST PROGRAM

Thirteen circular CFST beams and columns were tested to study the influence of bond upon their strength and load-deformation behavior. Both the loading regime and slenderness of the specimens were varied to cover the range from concentrically loaded stub columns through to beams. A summary of the test program is given in Table 1. Tests were also carried out on four companion empty steel tubes and seven unconfined concrete cylinders.

BOND CONDITIONS

Maximum bond

To maximize the transfer of shear between the inner surface of the circular steel tube and the infill concrete, 30-mm long x 4.9-mm hardened sheet metal self-tapping screws were inserted through holes in the wall of the tube prior to placement of the concrete. To avoid significantly weakening the steel tube as a whole, these screws were placed in a double helix pattern, with each helix having a pitch of 80 mm, as shown in Fig 1. Chemical bond between the steel and concrete was maximized by pickling the specimens in an acid bath followed by neutralizing in an alkaline bath.

Partial bond

An intermediate level of shear transfer was achieved by a thorough degreasing of the inside of each specimen in the as-received condition. This process insured some chemical bond to the factory-painted inner surface of the tube would be achieved, together with a limited amount of mechanical interlock due to its inherent surface roughness. This level of preparation reflects that undertaken in current construction practice.

Minimum bond

Chemical adhesion between the concrete and the inner surface of the steel tube in the as-received condition was minimized by

ACI Structural Journal, V. 96, No. 4, July-August 1999.
Received January 27, 1998, and reviewed under Institute publication policies.